

Observer Designs for Simultaneous Temperature and Loss Estimation for Electric Motors: A Comparative Study

Ma, Tong; Komatsu, Taiga; Wang, Bingnan; Wang, Yebin; Lin, Chungwei

TR2019-122 October 31, 2019

Abstract

Online temperature monitoring of electric motors is essential to the safety of the system under dynamic operation. The number of temperature sensors and their locations are often limited due to physical constraints and cost of the hardware, and the temperatures for most parts of a motor cannot be directly measured. To estimate the instantaneous temperature distribution of a motor, we design an observer for the real-time temperature monitoring using a thermal circuit model and limited measurements. Challenges imposed to the observer design include unknown heat sources and measurement noises. The observer needs to be able to simultaneously estimate all the hidden states and unknown inputs, while dealing with measurement noises. In this paper, different observers, including Kalman filter, Luenberger observer, adaptive observer, and modified proportional-derivative (PD) observer are designed to address the problem. We first give some background information of the problem, and introduce the thermal circuit model; then describe the observer designs with a focus on PD observer, which is more recently developed. The proposed observers are then implemented with simulations, and their performances are evaluated and compared.

IEEE Industrial Electronics Society (IECON) 2019

© 2019 MERL. This work may not be copied or reproduced in whole or in part for any commercial purpose. Permission to copy in whole or in part without payment of fee is granted for nonprofit educational and research purposes provided that all such whole or partial copies include the following: a notice that such copying is by permission of Mitsubishi Electric Research Laboratories, Inc.; an acknowledgment of the authors and individual contributions to the work; and all applicable portions of the copyright notice. Copying, reproduction, or republishing for any other purpose shall require a license with payment of fee to Mitsubishi Electric Research Laboratories, Inc. All rights reserved.

Observer Designs for Simultaneous Temperature and Loss Estimation for Electric Motors: A Comparative Study

Tong Ma*, Taiga Komatsu[†], Bingnan Wang*, Yebin Wang*, Chungwei Lin*

*Mitsubishi Electric Research Laboratories, 201 Broadway, Cambridge, MA 02139, USA

[†]Advanced R&D Center, Mitsubishi Electric Corp., 8-1-1 Tsukaguchihonmachi, Amagasaki, Hyogo, 661-8661, Japan

Abstract—Online temperature monitoring of electric motors is essential to the safety of the system under dynamic operation. The number of temperature sensors and their locations are often limited due to physical constraints and cost of the hardware, and the temperatures for most parts of a motor cannot be directly measured. To estimate the instantaneous temperature distribution of a motor, we design an observer for the real-time temperature monitoring using a thermal circuit model and limited measurements. Challenges imposed to the observer design include unknown heat sources and measurement noises. The observer needs to be able to simultaneously estimate all the hidden states and unknown inputs, while dealing with measurement noises. In this paper, different observers, including Kalman filter, Luenberger observer, adaptive observer, and modified proportional-derivative (PD) observer are designed to address the problem. We first give some background information of the problem, and introduce the thermal circuit model; then describe the observer designs with a focus on PD observer, which is more recently developed. The proposed observers are then implemented with simulations, and their performances are evaluated and compared.

Index Terms—Electric motor; estimation; inverse problem; measurement noise, observer.

I. INTRODUCTION

Temperature monitoring is critical in electric motor development and operation to avoid overheating, which affects the condition of the machine and causes various premature degradation and damages [1]. For example, the overheating of stator windings may lead to insulation failures; the overheating of permanent magnets may lead to irreversible demagnetization, etc. Installing temperature sensors in all the components, especially the rotating part, of a machine is either technically challenging, or prohibitively expensive. For example, in permanent magnet machines, the temperature of the permanent magnets has to be monitored closely; however, it is very difficult to measure the temperature directly.

On the other hand, the temperature rise in a motor is due to the “heat sources” in the motor which converts energy of other forms into thermal energy. Those heat sources include copper loss in windings, core loss in stator core, eddy current loss in permanent magnets, windage loss, and so on [2]. In practice it is very difficult to identify the heat sources completely, either by experimental measurements or theoretical modeling. For example, the core loss in iron laminations, mainly caused by the hysteresis loss and eddy current loss, can be affected by the motor manufacturing process. Theoretically, no existing model

can describe the process accurately. Experimentally, there is no good way to separate it apart from other heat sources.

The relationship between the heat sources and temperatures at each component of a motor can be described by heat equation. In practice, due to the complicated geometry, the heat equation can be solved with numerical methods such as finite-element simulations. Alternatively, it can be simplified with an equivalent thermal circuit model, or a lumped thermal circuit network [1], [2], where the circuit components, namely thermal resistances and thermal capacitances, are determined by the geometry and material properties of the motor. However, if the heat sources in the motor cannot be identified, the temperature distribution cannot be calculated.

In this work, we combine a thermal model of the motor with an estimator/observer and limited temperature measurements to simultaneously estimate the unknown heat sources and temperature distribution inside the motor. The proposed method is able to conduct the estimation in real-time, making it suitable for online condition monitoring for electric machines.

Solving joint estimation problem, e.g. online inverse heat transfer problem, we simultaneously identify the heat sources and temperatures based on the heat transfer model. Two main challenges arise when it comes to electric motors. First is due to measurement constraints. In practice only a few variables can be measured due to technical or economic reasons [3], and thus fails the detectability or observability test required in observer design. Additional constraints on input are incorporated into the thermal model to facilitate observer design. An insight on measurements’ dimension and location can be obtained by exploring the detectability or observability. Another challenge is that, the estimation accuracy will be greatly affected by measurement noise. An observer needs to be developed with limited measurements corrupted by noises.

Unknown input observer (UIO) [4] can achieve joint estimation of system states and unknown inputs under certain conditions. Early work of UIO design mainly focuses on the state estimation by avoiding the influence of the unknown inputs without reconstructing them. Later, the state estimation and unknown input reconstruction problems are considered. For example, the direct design procedure of full-order and reduced-order observer for linear systems with unknown inputs are presented in [5]–[7]. Refs. [8], [9] deal with the simultaneous state and input estimation problem based on

reduced-order observers. Recently, UIOs for switched linear systems are considered in [10], [11]. Handling of unknown disturbances is discussed in [12], [13]. Because the output is corrupted by measurement noise, measurement noise should be taken into consideration when evaluating the performance of observers. The problem of dealing with measurement noise is discussed in [14]–[18]. A modified proportional and derivative (PD) observer technique is presented to decouple the measurement noise and to obtain the estimation of the system states [14]. High-gain observer [15] switches between two gain values to recover the system states and to reduce the effect of measurement noise on estimation error. A high-gain observer with a gain adapted online can handle with measurement noise and uncertainties [16]. In [17], a reduced-order observer is designed to estimate the system states, and a kind of simultaneous reconstruction method of the unknown inputs and measurement noises is developed. [18] developed an L_1 adaptive descriptor for simultaneous estimation of all the hidden states, nonlinear uncertainties and measurement noises as well as delivering a good tracking performance.

By augmenting the state vector with unknown inputs, we first design Luenberger observer and Kalman Filter to solve the joint estimation problem as a state estimation problem. Second, by treating unknown inputs as parameters, the joint estimation problem is cast into a state and parameter estimation problem, for which an adaptive observer [19]–[22] is designed. Finally, a PD observer is designed to treat measurement noises [14]. For PD observer design, the original system should be detectable and measurement noise should be bounded. When solving our joint estimation problem, we augment the original system state with unknown inputs and measurement noise. In this approach, two design parameters provide additional degrees of freedom compared against Luenberger observer. The freedom of selecting these parameters allows us to choose the derivative gain to reduce the noise amplification, the proportional gain to ensure the stability of the estimation error dynamics.

The rest of the paper is organized as follows: Section II gives the description of the problem. In Section III different observers are designed for solving the online inverse heat transfer problem. The stability analysis of the error dynamics is given in Section IV for adaptive observer and PD observer. Numerical simulation results are demonstrated in Section V. A comparison is carried out to evaluate the performance of different observers, including the quantification of convergence speed and estimation error. Finally, the concluding remarks are given in Section VI.

II. PROBLEM DESCRIPTION

Figure 1 illustrates a quarter cross-section of an electric motor used in the study. The nodes, numbered 1 through 33, represent spatial locations where the temperature is of interest. By incorporating thermodynamics with red nodes, one can derive a thermal circuit network, where the temperature of each node, thermal flow between nodes, thermal conductivity,

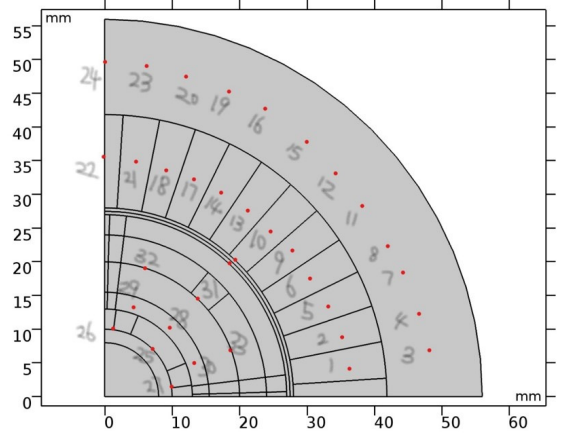


Fig. 1. Geometry of simplified electric motor.

and thermal capacity are analogous to voltage, current, resistance, and capacitance of an electric circuit network. Hence, the thermal circuit network induces dynamics of temperature at these locations, which can be fully described by the following multi-input multi-output (MIMO) thermal circuit model:

$$\begin{aligned} \dot{T}(t) &= AT(t) + Bu(t) + Vv \\ y_n(t) &= CT(t) + n(t) \end{aligned} \quad (1)$$

where $T \in R^n$ is the temperature at all nodes, $u(t) \in R^m$ contains the unknown heat sources, $y_n \in R^p$ is the measured temperature, $v \in R^{q \times 1}$ corresponds to temperatures at the boundary of the motor, and $n(t) \in R^p$ is the measurement noise. System matrices A, B, V, C are of appropriate dimensions.

The thermal circuit model (1) contains four unknown heat sources: u_1 -the stator iron loss, u_2 -the stator copper loss, u_3 -the rotor copper loss, and u_4 -the magnet loss. Specifically, u_1 is evenly distributed among nodes $\{1,5,9,13,17,21\}$; u_2 is evenly distributed among nodes $\{2,6,10,14,18,22\}$; u_3 is evenly distributed among nodes $\{25,26,27,31\}$; and u_4 is evenly distributed at nodes $\{28,29,30\}$. Our goal is to achieve joint estimation of temperature and heat sources in real time, which is abstracted as follows.

Problem 1: Given (1), construct a dynamical system as follows

$$\begin{aligned} \dot{\xi} &= f(\xi, y_n) \\ \hat{T} &= h_1(\xi, y_n) \\ \hat{u} &= h_2(\xi, y_n) \end{aligned}$$

where $\xi \in R^{n_\xi}$ such that ξ -dynamics are stable and $\lim_{t \rightarrow \infty} |T(t) - \hat{T}(t)| = 0$, $\lim_{t \rightarrow \infty} |u(t) - \hat{u}(t)| = 0$.

To solve Problem 1, without constraints, the number of sensors should be at least the same as the number of unknowns, which guarantees avoidance of the underdetermined cases. Besides that, for higher estimation accuracy, at least one sensor should be placed nearby each heat source. However, it is desired to avoid attaching sensors in the rotating parts due to technical difficulty and economic cost. To estimate the

temperature and heat loss distribution in the electric motor just using the measurements from stationary parts leads to the ill-conditioned problems. Hence, we want to explore some constraints that can help ease the problem. One reasonable assumption is that the total heat source can be identified by measuring the input electric power and output torque. Another constraint we can add is the stator winding loss, which can be measured by current and temperature sensors.

The constraints are formulated as below:

$$\begin{aligned} u_1(t) &= c_1 + 3\alpha T_1(t)I^2(t)R \\ \sum_{i=1}^m u_i(t) &= c_2 + 3\alpha T_1(t)I^2(t)R \end{aligned} \quad (2)$$

where $T_1(t)$ is the temperature of stator winding, α is the temperature coefficient of copper resistance, $I(t)$ is current, c_1 and c_2 are all known constants.

Since there are 4 inputs in total, denote

$$B = \begin{bmatrix} b_1 & b_2 & b_3 & b_4 \end{bmatrix} \quad (3)$$

where b_i is the corresponding column vector to input u_i ($i = 1, 2, 3, 4$).

Incorporating the constraints (2) into the circuit model defined in (1), a modified thermal model is derived as below:

$$\begin{aligned} \dot{T}(t) &= AT(t) + b_1 u_1(t) + Vv + (c_2 - 6c_1) b_4 \\ &+ \begin{bmatrix} b_2 - 6b_4 & b_3 - b_4 \end{bmatrix} \begin{bmatrix} u_2(t) \\ u_3(t) \end{bmatrix} \\ y_n(t) &= y(t) + n(t) \end{aligned} \quad (4)$$

After adding constraints, there are only two unknown heat sources in (4), u_2 and u_3 . Denote

$$B_m = \begin{bmatrix} b_2 - 6b_4 & b_3 - b_4 \end{bmatrix} \quad (5)$$

Since the thermal circuit model has been established, next step is to design observers for online estimation of the temperature and heat loss distribution in the electric motor.

III. OBSERVER DESIGN

Four observers, namely, Kalman filter, Luenberger observer, adaptive observer, and PD observer, are designed for Problem 1. Note that the observer design is developed on the basis of general linear time-invariant (LTI) systems (1). Observers design for the specific online inverse heat transfer problem stated in (4) will be given in Section V.

For simplicity, we introduce the following assumption.

Assumption 2: Unknown heat losses $u(t)$ are constant.

Given Assumption 2, one can augment the state T in (1) by treating u as states, and have the following extended state-space model

$$\begin{aligned} \begin{bmatrix} \dot{T}(t) \\ \dot{u}(t) \end{bmatrix} &= A_e \begin{bmatrix} T(t) \\ u(t) \end{bmatrix} + V_e v \\ y_n(t) &= C_e \begin{bmatrix} T(t) \\ u(t) \end{bmatrix} + n(t) \end{aligned} \quad (6)$$

where

$$\begin{aligned} A_e &= \begin{bmatrix} A & B \\ 0_{m \times n} & 0_{m \times m} \end{bmatrix}, \quad V_e = \begin{bmatrix} V \\ 0_{m \times q} \end{bmatrix} \\ C_e &= \begin{bmatrix} C & 0_{p \times m} \end{bmatrix}. \end{aligned}$$

Denote

$$C_o = \begin{bmatrix} A_e \\ C_e \end{bmatrix} \quad (7)$$

Since the output matrix C contains the information of measurements' size and location, the design of C should satisfy the detectability requirement and it needs to be determined before the observer design. For the determination of measurements' size and location, check the rank and singular values of the matrix C_o . If $\text{rank}(C_o) = n + m$, and all the singular values are non-zeros, then the observer will work well with the designed C . Even though $\text{rank}(C_o) = n + m$, if there exist some singular values equal to zeros or are almost zeros, it means there exist some modes in the system are difficult to be detected, it is time-consuming to tune such an observer for higher estimation accuracy.

A. Luenberger Observer

Given Eq. 6, a Luenberger observer can be designed to estimate $T(t)$ and $u(t)$ simultaneously. Its dynamics are formulated as below:

$$\begin{aligned} \begin{bmatrix} \dot{\hat{T}}(t) \\ \dot{\hat{u}}(t) \end{bmatrix} &= \begin{bmatrix} A & B \\ 0 & 0 \end{bmatrix} \begin{bmatrix} \hat{T}(t) \\ \hat{u}(t) \end{bmatrix} + \begin{bmatrix} V \\ 0_{m \times q} \end{bmatrix} v \\ &+ K \left(y_n(t) - C\hat{T}(t) \right) \end{aligned} \quad (8)$$

where \hat{T} and \hat{u} denotes estimate of T and u respectively. The resultant estimation error dynamics are

$$\begin{bmatrix} \dot{\tilde{T}}(t) \\ \dot{\tilde{u}}(t) \end{bmatrix} = (A_e - KC_e) \begin{bmatrix} \tilde{T}(t) \\ \tilde{u}(t) \end{bmatrix} + Kn(t) \quad (9)$$

where $\tilde{T} = T - \hat{T}$, $\tilde{u} = u - \hat{u}$. From linear control theory, the estimation error dynamics (9) are stable if and only if the pair (A_e, C_e) is detectable. The error dynamics (9) are evidently affected by the measurement noise.

B. Kalman filter

Different from Luenberger observer, Kalman filter (KF) offers an elegant treatment of uncertainties in measurements and process. For linear dynamical systems, KF produces optimal estimates in the sense of minimal covariance of estimation error. Next we briefly describe the steps to apply KF to the model (6).

We discretize (6) to have its discrete-time representation

$$\begin{aligned} \begin{bmatrix} T_k \\ u_k \end{bmatrix} &= F_k \begin{bmatrix} T_{k-1} \\ u_{k-1} \end{bmatrix} + \begin{bmatrix} V_k \\ 0_{m \times q} \end{bmatrix} v_k + w_k \\ z_k &= H_k \begin{bmatrix} T_k \\ u_k \end{bmatrix} + n_k \end{aligned} \quad (10)$$

where F_k is the discrete-time transition matrix. The priori prediction step is given as below:

$$\begin{bmatrix} \hat{T}_{k|k-1} \\ \hat{u}_{k|k-1} \end{bmatrix} = F_k \begin{bmatrix} \hat{T}_{k-1|k-1} \\ \hat{u}_{k-1|k-1} \end{bmatrix} + \begin{bmatrix} V_k \\ 0_{m \times q} \end{bmatrix} v_k$$

$$P_{k|k-1} = \text{cov} \left(\begin{bmatrix} T_k \\ u_k \end{bmatrix} - \begin{bmatrix} \hat{T}_{k|k-1} \\ \hat{u}_{k|k-1} \end{bmatrix} \right) \quad (11)$$

$$= F_k P_{k-1|k-1} F_k^T + Q_k$$

where $P_{k|k-1}$ is the predicted error covariance. A posterior correction updates the state and covariance as below

$$\tilde{y}_k = z_k - H_k \begin{bmatrix} \hat{T}_{k|k-1} \\ \hat{u}_{k|k-1} \end{bmatrix}$$

$$K_k = (F_k P_{k-1|k-1} F_k^T + Q_k) H_k^T (R_k + H_k (F_k P_{k-1|k-1} F_k^T + Q_k) H_k^T)^{-1}$$

$$\begin{bmatrix} \hat{T}_{k|k} \\ \hat{u}_{k|k} \end{bmatrix} = \begin{bmatrix} \hat{T}_{k|k-1} \\ \hat{u}_{k|k-1} \end{bmatrix} + K_k \tilde{y}_k$$

$$P_{k|k} = \text{cov} \left(\begin{bmatrix} T_k \\ u_k \end{bmatrix} - \begin{bmatrix} \hat{T}_{k|k} \\ \hat{u}_{k|k} \end{bmatrix} \right)$$

$$= (I - K_k H_k) (F_k P_{k-1|k-1} F_k^T + Q_k) (I - K_k H_k)^T + K_k R_k K_k^T \quad (12)$$

where \tilde{y}_k is the measurement residual, K_k is the optimal Kalman gain, and $P_{k|k}$ is the updated estimate covariance. KF yields stable estimation error dynamics if and only if (A_e, C_e) is detectable.

C. Adaptive observer

Adaptive observers are widely used for state and parameter estimation which enables adaptive control or fault estimation in fault detection and isolation [24]. By viewing u as unknown parameters, one can readily solve Problem 1 by applying existing linear adaptive observer design results.

First, we split the state T into two components T_1 and T_2 , which corresponds to known v and unknown excitation u respectively. Their dynamics are derived as below:

$$\begin{aligned} \dot{T}_1(t) &= (A - KC) T_1(t) + Vv + Ky(t) \\ \dot{T}_2(t) &= (A - KC) T_2(t) + Bu(t) \end{aligned} \quad (13)$$

The estimators for the subsystems in (13) are given by

$$\begin{aligned} \dot{\hat{T}}_1(t) &= (A - KC) \hat{T}_1(t) + Vv + Ky_n(t) \\ \dot{\hat{T}}_2(t) &= (A - KC) \hat{T}_2(t) + B\hat{u}(t) + \sigma(t) \end{aligned} \quad (14)$$

where $\hat{u}(t)$ is an estimate of unknown $u(t)$, and $\sigma(t)$ compensates the estimation error caused by $\hat{u}(t)$. Since the subsystem \hat{T}_2 is excited by \hat{u} and $\hat{T}_2(0) = 0$, we know

$$\hat{T}_2(t) = \gamma(t) \hat{u}(t) \quad (15)$$

Substitute (15) into (14), we can derive:

$$\dot{\gamma}(t) = (A - KC) \gamma(t) + B, \quad \sigma(t) = \gamma(t) \dot{\hat{u}}(t) \quad (16)$$

Eventually, we have the adaptive observer as follows

$$\begin{aligned} \dot{\hat{T}}(t) &= A\hat{T}(t) + B\hat{u}(t) + K \left(y_n(t) - C\hat{T}(t) \right) \\ &\quad + \gamma(t) \dot{\hat{u}}(t) + Vv \end{aligned} \quad (17)$$

$$\dot{\hat{u}}(t) = \Gamma \gamma^T(t) C^T \Sigma \left(y_n(t) - C\hat{T}(t) \right) \quad (18)$$

The resultant estimation error dynamics are as below:

$$\begin{aligned} \dot{\tilde{T}}(t) &= (A - KC) \tilde{T}(t) + B\tilde{u}(t) + \gamma(t) \dot{\tilde{u}}(t) + Kn(t) \\ \dot{\tilde{u}}(t) &= -\Gamma \gamma^T(t) C^T \Sigma \left(y_n(t) - C\hat{T}(t) \right) \end{aligned} \quad (19)$$

Stability analysis of (19) is a little trickier than that of KF and Luenberger observer, and we leave it to the next section.

D. PD Observer

PD observer is proposed for systems with measurement noises. It estimates all states, unknown inputs and measurement noises at the same time. The model (6) is further extended by including the noise $n(t)$ as state, which gives the following dynamics

$$\bar{E} \dot{\bar{x}}(t) = \bar{A} \bar{x}(t) + \begin{bmatrix} V \\ 0_{(m+p) \times q} \end{bmatrix} v + \bar{N} n_{p \times 1}(t) \quad (20)$$

$$y_n(t) = \bar{C} \bar{x}(t)$$

where

$$x_n(t) = n_{p \times 1}(t), \quad \bar{x}(t) = \begin{bmatrix} T(t) \\ u(t) \\ x_n(t) \end{bmatrix},$$

$$\bar{N} = \begin{bmatrix} 0 \\ I_p \end{bmatrix}, \quad \bar{E} = \begin{bmatrix} I_{n+m} & 0_{(n+m) \times p} \\ 0_{p \times (n+m)} & 0_{p \times p} \end{bmatrix}, \quad (21)$$

$$\bar{A} = \begin{bmatrix} A_e & 0_{(n+m) \times p} \\ 0_{p \times (n+m)} & -I_p \end{bmatrix},$$

$$\bar{C} = [C \quad 0_{p \times m} \quad I_p]$$

Given (20), PD observer is derived as below:

$$\begin{aligned} (\bar{E} + \bar{L}\bar{C}) \dot{\xi}(t) &= (\bar{A} - \bar{K}\bar{C}) \xi(t) + \begin{bmatrix} V \\ 0_{(m+p) \times q} \end{bmatrix} v \\ &\quad + \bar{A} (\bar{E} + \bar{L}\bar{C})^{-1} \bar{L} y_n(t) \\ \hat{\hat{x}}(t) &= \xi(t) + (\bar{E} + \bar{L}\bar{C})^{-1} \bar{L} y_n(t) \end{aligned} \quad (22)$$

where $\bar{L}, \bar{K} \in R^{(n+m+p) \times p}$ are gain matrices, and $\hat{\hat{x}}(t)$ is the estimation of $\bar{x}(t)$ in (20). PD observer for Problem 1 is depicted in Figure 2.

Compared with Luenberger observer, PD observer introduces two design parameters \bar{L} and \bar{K} which offer better tradeoff between the convergence rate of the observer and the robustness to the measurement noise. In fact, the derivative gain \bar{L} is chosen to minimize the amplification of the measurement noise, and the proportional gain \bar{K} is selected to guarantee the stability of the error dynamics. As shown in the next section, if the matrix pair (A_e, C_e) is detectable and the noise is bounded, these two design parameters will provide more degrees of freedom.

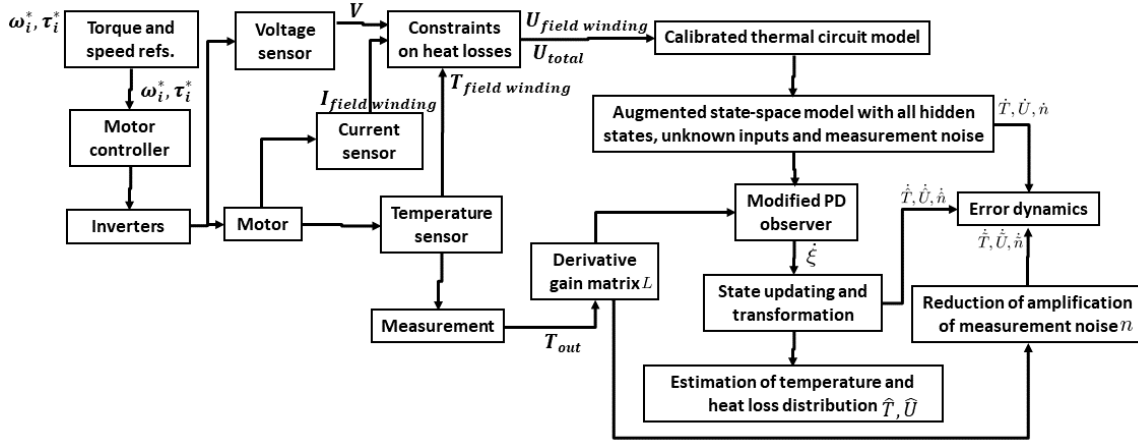


Fig. 2. Diagram of PD observer for Problem 1

IV. ANALYSIS

Stability analysis of the error dynamics result from PD observer and adaptive observer is presented in this section.

A. Adaptive Observer

We first introduce a notation

$$\eta(t) = \tilde{T}(t) - \gamma(t)\tilde{u}(t) \quad (23)$$

Substitute (23) into (19), we have

$$\begin{aligned} \dot{\eta}(t) &= (A - KC)\eta(t) + Kn(t) \\ \dot{\tilde{u}}(t) &= -\Gamma\gamma^T(t)C^T\Sigma C(\gamma(t)\tilde{u}(t) + \eta(t)) + \Gamma\gamma^T(t)C^T\Sigma n(t) \end{aligned} \quad (24)$$

Stability of (24) depends on the following two Assumptions

Assumption 3: The matrix pair (A, C) is detectable.

Assumption 4: For $\dot{\gamma}(t) = (A - KC)\gamma(t) + B$, there exist positive constants α, β, T such that $\forall t > 0$,

$$\alpha I \leq \int_t^{t+T} \gamma^T(\tau)C^T\Sigma(\tau)C\gamma(\tau)d\tau \leq \beta I \quad (25)$$

is satisfied.

Recalling stability analysis in [24], one can establish that (24) are exponentially stable if Assumptions 3 and 4 hold.

B. PD Observer

First, we will give the following theorem [14].

Theorem 5: If the matrix pair (A_e, C_e) is detectable and the noise is bounded, there exist the gain matrices $\bar{L}, \bar{K} \in R^{(n+m+p) \times p}$ for the observer defined in Eq. 22, such that $\hat{x}(t)$ is an asymptotic estimate of $\bar{x}(t)$ in (20).

Proof : Notice that

$$\begin{aligned} \text{rank} \begin{bmatrix} \bar{E} \\ \bar{C} \end{bmatrix} &= \text{rank} \begin{bmatrix} I_{n+m} & 0_{(n+m) \times p} \\ 0_{p \times (n+m)} & 0_{p \times p} \\ C_e & I_p \end{bmatrix} \\ &= n + m + p \end{aligned} \quad (26)$$

then there exists $\bar{L} \in R^{(n+m+p) \times p}$ such that $\text{rank}(\bar{E} + \bar{L}\bar{C}) = n + m + p$, which means $(\bar{E} + \bar{L}\bar{C})$ is invertible.

For explicit $(\bar{E} + \bar{L}\bar{C})$, write $\bar{L} = \begin{bmatrix} L_1 \\ L_2 \end{bmatrix}$, where $L_1 \in R^{(n+m) \times p}$, $L_2 \in R^{p \times p}$, it can be shown that

$$\bar{C}(\bar{E} + \bar{L}\bar{C})^{-1}\bar{L} = I_p \quad (27)$$

Substituting $\xi(t) = \hat{x}(t) - (\bar{E} + \bar{L}\bar{C})^{-1}\bar{L}y_n(t)$ into Eq. 22 and using Eq. 27, we can derive

$$\begin{aligned} (\bar{E} + \bar{L}\bar{C})\dot{\hat{x}}(t) &= (\bar{A} - \bar{K}\bar{C})\hat{x}(t) \\ &+ \begin{bmatrix} V \\ 0_{(m+p) \times q} \end{bmatrix} v + \bar{K}y_n(t) + \bar{L}\dot{y}_n(t) \end{aligned} \quad (28)$$

Adding $L\dot{y}(t)$ to both sides of (20), we get

$$\begin{aligned} (\bar{E} + \bar{L}\bar{C})\dot{\hat{x}}(t) &= (\bar{A} - \bar{K}\bar{C})\hat{x}(t) + \begin{bmatrix} V \\ 0_{(m+p) \times q} \end{bmatrix} v \\ &+ \bar{K}y_n(t) + \bar{L}\dot{y}_n(t) + \bar{N}n_{p \times 1}(t) \end{aligned} \quad (29)$$

The error dynamics is formulated as below based on (28) and (29):

$$\dot{\hat{e}}(t) = (\bar{E} + \bar{L}\bar{C})^{-1}(\bar{A} - \bar{K}\bar{C})\hat{e}(t) + (\bar{E} + \bar{L}\bar{C})^{-1}\bar{N}n_{p \times 1}(t) \quad (30)$$

The term which contains measurement noise in (30) can be written as below:

$$(\bar{E} + \bar{L}\bar{C})^{-1}\bar{N}n_{p \times 1}(t) = \begin{bmatrix} -L_1 \\ I_p + CL_1 \end{bmatrix} (L_2)^{-1}n_{p \times 1}(t) \quad (31)$$

As we can see from (31), a low gain L_1 , for example, $L_1 = 0$, and a high-gain L_2 can be chosen to reduce the amplification of measurement noise.

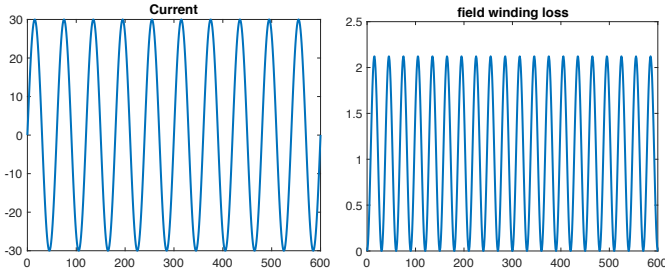


Fig. 3. Current and field winding loss in the electric motors.

After doing some matrix computation, we have

$$\begin{aligned}
& \text{rank} \left[sI_{n+m+p} - \begin{bmatrix} \bar{E} + \bar{L}\bar{C} \\ \bar{C} \end{bmatrix}^{-1} \bar{A} \right] \\
&= \text{rank} \left[s \begin{bmatrix} \bar{E} + \bar{L}\bar{C} \\ \bar{C} \end{bmatrix} - \bar{A} \right] \\
&= \text{rank} \begin{bmatrix} s\bar{E} - \bar{A} \\ \bar{C} \end{bmatrix} \\
&= \text{rank} \begin{bmatrix} sI_{n+m} - A_e & 0_{(n+m) \times p} \\ 0_{p \times (n+m)} & I_p \\ & C_e & I_p \end{bmatrix} \\
&= \text{rank} \left[sI_{n+m} - \begin{bmatrix} A & B \\ 0 & 0 \end{bmatrix} \right] + p
\end{aligned} \tag{32}$$

If (A_e, C_e) is detectable, (32) means that $\left(\begin{bmatrix} \bar{E} + \bar{L}\bar{C} \\ \bar{C} \end{bmatrix}^{-1} \bar{A}, \bar{C} \right)$ is detectable. Then we can select \bar{K}^* such that $\left[\begin{bmatrix} \bar{E} + \bar{L}\bar{C} \\ \bar{C} \end{bmatrix}^{-1} \bar{A} - \bar{K}^* \bar{C} \right]$ is a Hurwitz matrix, and $\bar{K} = \begin{bmatrix} \bar{E} + \bar{L}\bar{C} \\ \bar{C} \end{bmatrix}^{-1} \bar{K}^*$.

V. SIMULATION

In this section, different observers are implemented for the online estimation of temperature and heat source distribution in electric motors. For the specified online inverse heat transfer problem, $u_1(t)$ is time-varying, random measurement noise between -1°C and 1°C are added. The current and field winding loss are shown in Figure 3.

A. Sensor placement

Since u_2 and u_3 are unknown inputs, they can be taken as state variables. The extended state-space model is established as in (4). In this case, $A_e = \begin{bmatrix} A & B_m \\ 0 & 0 \end{bmatrix}$, $C_e = \begin{bmatrix} C & 0 \end{bmatrix}$, $C_o = \begin{bmatrix} A & B_m \\ C & 0 \end{bmatrix}$. For the determination of measurements' size and location, check the rank and singular values of the matrix C_o . If $\text{rank}(C_o) = n + 2$, and all the singular values are non-zeros, then the observer will work well with the designed C .

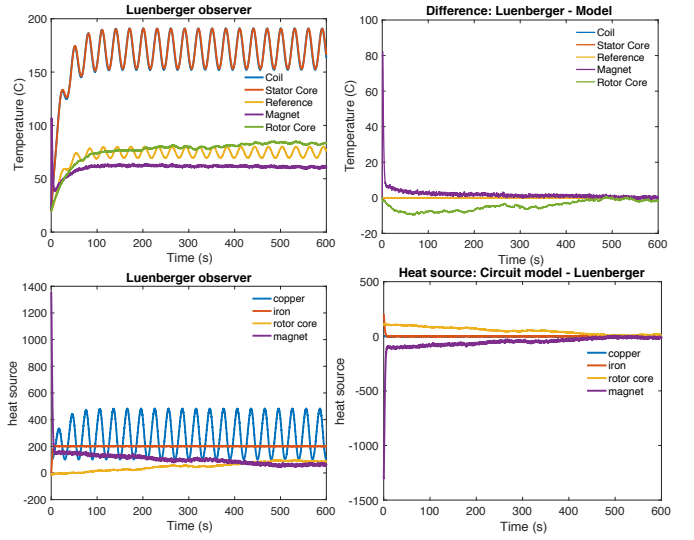


Fig. 4. Online estimation of temperature and heat loss distribution in electric motors using Luenberger observer.

B. Luenberger observer

Based on (4), the Luenberger observer is formulated as below:

$$\begin{aligned}
\begin{bmatrix} \hat{T}(t) \\ \hat{u}_2(t) \\ \hat{u}_3(t) \end{bmatrix} &= \begin{bmatrix} A & B_m \\ 0 & 0 \end{bmatrix} \begin{bmatrix} \hat{T}(t) \\ \hat{u}_2(t) \\ \hat{u}_3(t) \end{bmatrix} + Vv \\
&+ b_1 u_1(t) + K \left(y_n(t) - C\hat{T}(t) \right) + (c_2 - 6c_1) b_4
\end{aligned} \tag{33}$$

The numerical simulation results for online estimation of temperature and heat loss distribution in electric motors using Luenberger observer is shown in Figure 4. The left figure on the top shows the temperature estimation results using the Luenberger observer, in this figure, we pick up one node from the coil, stator core, magnet, rotor core, respectively. "Reference" is one of the nodes where the sensors are located. The right figure on the top shows the temperature estimation errors between the Luenberger observer and circuit model. The left figure below shows the reconstruction results of the heat loss distribution in the electric motor using Luenberger observer, including the copper loss, iron loss, rotor core loss, and magnet loss. The right figure below shows the heat loss estimation errors between the Luenberger observer and circuit model. As we can see from Figure 4, the estimation results are corrupted by measurement noises using Luenberger observer, which is evident from (9).

C. Kalman filter

The numerical simulation results for online estimation of temperature and heat loss distribution in electric motors using kalman filter are shown in Figure 5. As we can see from Figure 5, the estimation results are corrupted by measurement noises using Kalman filter, which can be seen from (12).

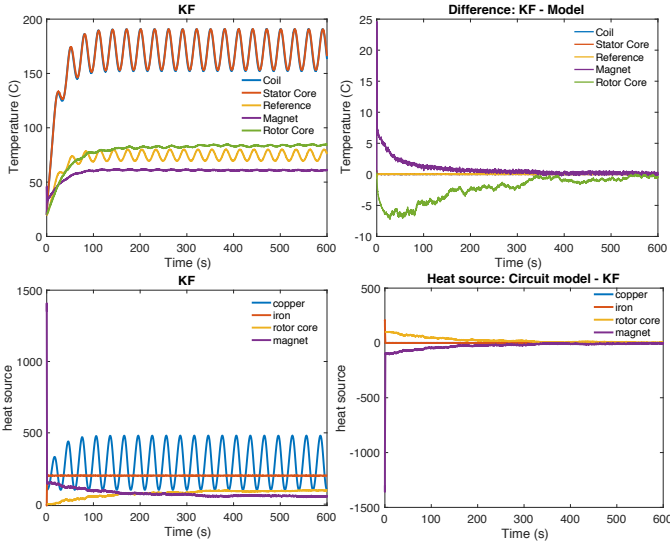


Fig. 5. Online estimation of temperature and heat loss distribution in electric motors using kalman filter.

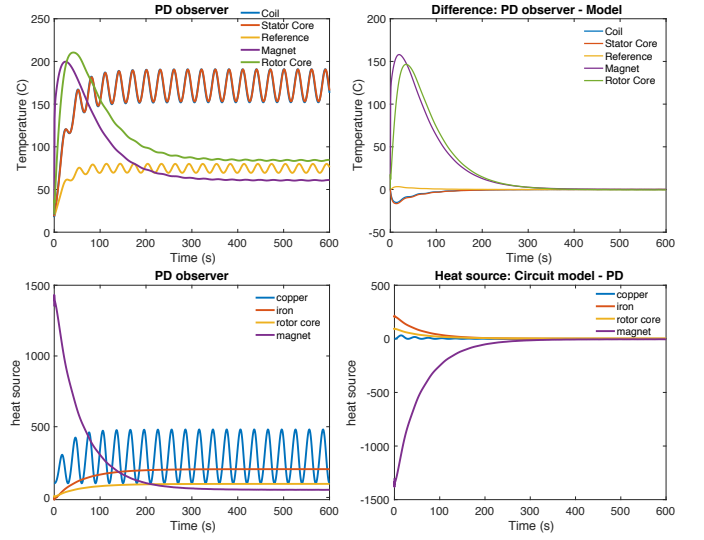


Fig. 7. Online estimation of temperature and heat loss distribution in electric motors using PD observer.

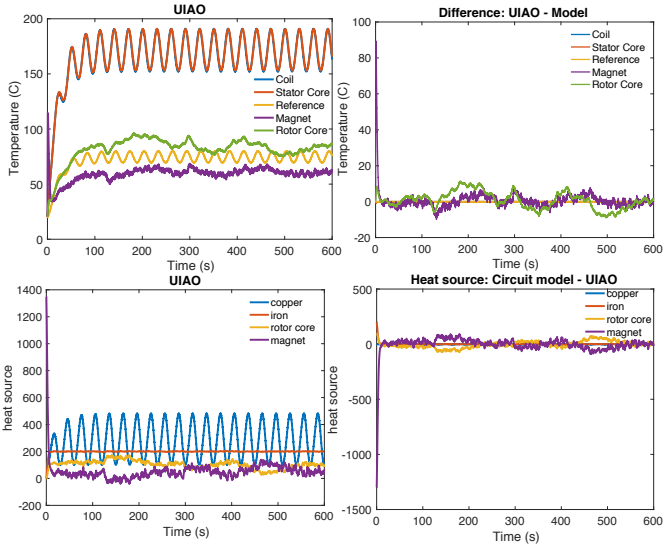


Fig. 6. Online estimation of temperature and heat loss distribution in electric motors using adaptive observer.

D. Adaptive observer

The adaptive observer for the specific inverse heat transfer problem (4) is formulated as below:

$$\begin{aligned} \dot{\hat{T}}(t) &= A\hat{T}(t) + B_m\hat{u}(t) + K \left(y_n(t) - C\hat{T}(t) \right) + \\ &\gamma(t)\dot{\hat{u}}(t) + b_1u_1(t) + Vv + (c_2 - 6c_1)b_4 \end{aligned} \quad (34)$$

$$\dot{\hat{u}}(t) = \Gamma\gamma^T(t)C^T\Sigma \left(y_n(t) - C\hat{T}(t) \right) \quad (35)$$

The numerical simulation results for online estimation of temperature and heat loss distribution in electric motors using adaptive observer are shown in Figure 6. As we can see from Figure 6, the estimation results are corrupted by measurement noises using adaptive observer, which is evident from (19).

E. PD observer

The PD observer is designed to estimate all the hidden states, unknown inputs and measurement noises at the same time. The extended state-space model is given as below:

$$\begin{aligned} \bar{E}\dot{\bar{x}}(t) &= \bar{A}\bar{x}(t) + \begin{bmatrix} b_1 \\ 0_{(m+p) \times 1} \end{bmatrix} u_1(t) + \begin{bmatrix} V \\ 0_{(m+p) \times 2} \end{bmatrix} v \\ &+ \begin{bmatrix} (c_2 - 6c_1)b_4 \\ 0_{(m+p) \times 1} \end{bmatrix} + \bar{N}n_{p \times 1}(t) \\ y_n(t) &= \bar{C}\bar{x}(t) \end{aligned} \quad (36)$$

If the matrix (A_e, C_e) is detectable and the noise is bounded, a modified PD observer for online estimation of temperature and heat loss distribution in the electric motors is derived as below:

$$\begin{aligned} (\bar{E} + \bar{L}\bar{C})\dot{\xi}(t) &= (\bar{A} - \bar{K}\bar{C})\xi(t) + \begin{bmatrix} b_1 \\ 0_{(m+p) \times 1} \end{bmatrix} u_1(t) \\ &+ \begin{bmatrix} V \\ 0_{(m+p) \times 2} \end{bmatrix} v + \begin{bmatrix} (c_2 - 6c_1)b_4 \\ 0_{(m+p) \times 1} \end{bmatrix} \\ &+ \bar{A}(\bar{E} + \bar{L}\bar{C})^{-1}\bar{L}y_n(t) \end{aligned} \quad (37)$$

$$\hat{\bar{x}}(t) = \xi(t) + (\bar{E} + \bar{L}\bar{C})^{-1}\bar{L}y_n(t) \quad (38)$$

where $\hat{\bar{x}}(t)$ is an asymptotic estimation of $\bar{x}(t)$ in (36).

The numerical simulation results for online estimation of temperature and heat loss distribution in electric motors using modified PD observer are shown in Figure 7.

In terms of different observers design, Luenberger observer is well known for output feedback of linear time-invariant systems. Adaptive observer is often used for joint estimation of hidden states and unknown parameters. Kalman filter has the

optimal performance for linear time-invariant systems. Without the presence of measurement noise, asymptotic estimation of temperature field and heat loss distribution is achieved. Since none of these three observers has something to do with the measurement noise, the estimation results will be corrupted by the measurement noise, as we can see in (9). As for the PD observer, under the condition where the system is detectable and the measurement noise is bounded, there exist two design parameters which can provide more degrees of freedom. The derivative gain is chosen to minimize the amplification of the measurement noise, and the proportional gain is selected to guarantee the stability of the error dynamics. Hence, the PD observer can almost reject the measurement noise completely with properly chosen parameters. Actually, the choice of derivative gain is a trade-off between convergence speed and estimation error for PD observer. A larger derivative gain will reduce the amplification of measurement noise greatly, but the convergence speed is really slow; a smaller gain will speed up the convergence process, but the estimation error caused by measurement noise is amplified.

VI. CONCLUSIONS

Different observers are designed for real-time estimation of temperature and heat loss distribution in electric motors. In view of the ill-posedness of the problem, physical constraints are imposed to remedy the limitation. Insights on measurements' size and location are provided by exploring the detectability of the observer. Since the measurements are corrupted by noises, the estimation accuracy will be greatly affected in some cases, hence, measurement noises are taken into consideration for estimation error analysis. In terms of different observers design, Luenberger observer is well known for output feedback of linear time-invariant systems. Adaptive observer is often used for joint estimation of hidden states and unknown parameters. Kalman filter has the optimal performance for linear time-invariant systems. As for PD observer, it can reject the measurement noise to some extent. Actually, the choice of derivative gain is a trade-off between convergence speed and estimation error for PD observer. A larger derivative gain significantly reduces the amplification of measurement noise greatly, at the cost of convergence speed; a smaller gain will speed up the convergence process, but the estimation error caused by measurement noise is amplified.

REFERENCES

- [1] R. Saheba, M. Rotea, O. Wasynczuk, S. Pekarek and B. Jordan, "Virtual Thermal Sensing for Electric Machines," in *IEEE Control Systems Magazine*, vol. 30, no. 1, pp. 42-56, Feb. 2010.
- [2] J. Pyrhonen, T. Jokinen, and V. Hrabovcova, *Design of rotating electrical machines*. John Wiley & Sons, 2013.
- [3] H. K. Khalil, "Nonlinear systems," Prentice-Hall, New Jersey, vol. 2, pp. 5-1, 1996.
- [4] J. Yang, F. Zhu, and X. Sun, "State estimation and simultaneous unknown input and measurement noise reconstruction based on associated observers," *International Journal of Adaptive Control and Signal Processing*, vol. 27, pp. 846-858, 2013.
- [5] F. Yang and R. W. Wilde, "Observers for linear systems with unknown inputs," *IEEE Transactions on Automatic Control*, vol. 33, pp. 677-681, 1988.
- [6] Hou, Mller, and P. C. Muller. "Design of observers for linear systems with unknown inputs." *IEEE Transactions on Automatic Control* 37, no. 6 (1992): 871-875.
- [7] M. Darouach, M. Zasadzinski, and S. J. Xu, "Full-order observers for linear systems with unknown inputs," *IEEE Transactions on Automatic Control*, vol. 39, pp. 606-609, 1994.
- [8] H. Trinh and Q. P. Ha, "State and input simultaneous estimation for a class of time-delay systems with uncertainties," *IEEE Transactions on Circuits and Systems II: Express Briefs*, vol. 54, pp. 527-531, 2007.
- [9] H. Trinh, T. D. Tran, and T. Fernando, "Disturbance decoupled observers for systems with unknown inputs," *IEEE Transactions on Automatic control*, vol. 53, pp. 2397-2402, 2008.
- [10] F. J. Bejarano and L. Fridman, "State exact reconstruction for switched linear systems via a super-twisting algorithm," *International Journal of Systems Science*, vol. 42, pp. 717-724, 2011.
- [11] F. J. Bejarano and A. Pisano, "Switched observers for switched linear systems with unknown inputs," *IEEE Transactions on Automatic Control*, vol. 56, pp. 681-686, 2011.
- [12] R. Marino and G. L. Santosuosso, "Global compensation of unknown sinusoidal disturbances for a class of nonlinear nonminimum phase systems," *IEEE Transactions on Automatic Control*, vol. 50, pp. 1816-1822, 2005.
- [13] S. Aranovskiy and A. Bobtsov, "Output harmonic disturbance compensation for nonlinear plant," in *Control & Automation (MED), 2012 20th Mediterranean Conference on*, 2012, pp. 386-391.
- [14] Z. Gao and H. Wang, "Descriptor observer approaches for multivariable systems with measurement noises and application in fault detection and diagnosis," *Systems & Control Letters*, vol. 55, pp. 304-313, 2006.
- [15] J. H. Ahrens and H. K. Khalil, "High-gain observers in the presence of measurement noise: A switched-gain approach," *Automatica*, vol. 45, pp. 936-943, 2009.
- [16] R. G. Sanfelice and L. Praly, "On the performance of high-gain observers with gain adaptation under measurement noise," *Automatica*, vol. 47, pp. 2165-2176, 2011.
- [17] Z. Gao, T. Breikin, and H. Wang, "High-gain estimator and fault-tolerant design with application to a gas turbine dynamic system," *IEEE Transactions on Control Systems Technology*, vol. 15, pp. 740-753, 2007.
- [18] Ma, Tong, and Chengyu Cao. "L1 adaptive outputfeedback descriptor for multivariable nonlinear systems with measurement noises." *International Journal of Robust and Nonlinear Control*.
- [19] A. K. Caglayan and R. E. Lancraft, "A separated bias identification and state estimation algorithm for nonlinear systems," *Automatica*, vol. 19, pp. 561-570, 1983.
- [20] R. Marino and P. Tomei, "Adaptive observers with arbitrary exponential rate of convergence for nonlinear systems," *IEEE Transactions on Automatic Control*, vol. 40, pp. 1300-1304, 1995.
- [21] R. Marino and P. Tomei, *Nonlinear control design: geometric, adaptive and robust vol. 1*: Prentice Hall London, 1995.
- [22] H. Wang and S. Daley, "Actuator fault diagnosis: an adaptive observer-based technique," *IEEE Transactions on Automatic Control*, vol. 41, pp. 1073-1078, 1996.
- [23] P. A. Ioannou and J. Sun, *Robust adaptive control vol. 1*: PTR Prentice-Hall Upper Saddle River, NJ, 1996.
- [24] Q. Zhang, "Adaptive observer for multiple-input-multiple-output (MIMO) linear time-varying systems," *IEEE Transactions on Automatic Control*, vol. 47, pp. 525-529, 2002.